Journal of the Physical Society of Japan
Vol. 77, No. 8, August, 2008, 084703

First-Principles Study of BN, SiC, and AlN Polytypes

Kazuaki KOBAYASHI and Shojiro KOMATSU

National Institute for Materials Science, 1-1 Namiki, Tsukuba, Ibaraki 305-0044

(Received December 27, 2007; accepted June 2, 2008; published July 25, 2008)

We calculated the electronic and lattice properties of BN, SiC, and AlN polytypes. The calculated polytypes are 2H, 3C (= 3H), 4H, 5H, and 6H. These polytypes are sp^3-bonded compounds. The 6H polytype has two crystal structures as ABCACB and ABCBCB stacking sequences. The lattice properties were optimized automatically by the first-principles molecular dynamics (FPMD) method. Most calculated electronic band structures of these polytypes are non-metallic and their band gaps are indirect. The most stable BN, SiC and AlN polytypes are 3C-BN, 4H-SiC, and 2H-AlN, respectively. The calculated total energies of BN polytypes are in the order of 3C < 6H(ABCACB) < 5H < 4H < 6H(ABCBCB) < 2H. The calculated total energies of SiC polytypes are in the order of 4H < 6H(ABCACB) < 3C < 5H < 6H(ABCBCB) < 2H. The calculated total energies of AlN polytypes are in the order of 2H < 6H(ABCBCB) < 4H < 5H < 6H(ABCACB) < 3C. The total energies and energetical stabilities of the BN and AlN polytypes are related to hexagonality which corresponds to the ratio of the number of third-neighbor cation–anion pairs and the number of cation–anion bilayers in the unit cell. 6H-BN(ABCACB) and 6H-SiC(ABCACB) are energetically more favorable than 6H-BN(ABCBCB) and 6H-SiC(ABCBCB), respectively. In contrast, 6H-AlN(ABCBCB) is more favorable than 6H-AlN(ABCACB).

KEYWORDS: polytype, BN, SiC, AlN, first-principles, electronic band structure
DOI: 10.1143/JPSJ.77.084703

1. Introduction

5H-boron nitride (BN) is a new material that has been synthesized by Komatsu *et al.*[1–4] 5H-BN is one of various polytypes[5–7] which consists of hexagonal boron and nitrogen layers in a unit cell. It is an sp^3-bonded BN compound which is different from sp^2-bonded compounds such as hexagonal- and rhombohedral-BN (*h*- and *r*-BN). Although there are many theoretical[8–12] and experimental[13] studies of BN compounds, there are no theoretical studies of 5H-BN with the exception of our previous study in which we investigated the electronic and lattice properties of 5H-BN.[14] The calculated lattice properties of 5H-BN agree well with experimental results[1] and the electronic properties have been definitively established. In the previous study,[14] we also calculated the electronic properties of 2H-, 3H-(= 3C-), and 4H-BN. These are polytypes which are also sp^3-bonded hexagonal layered structures. 2H- and 3C-BN are important sp^3-bonded compounds with wide band gaps. 2H-BN is synthesized by compression or shock compression[13] and its crystal structure is wurtzite. 3C-BN whose crystal structure is zinc-blende is also synthesized by compression.[13] Energetically, 3C-BN was most stable in the previous study.[14] There are a few studies of 4H-BN[15,16] and a few of 6H-BN.[1,17] Their lattice and electronic properties have not been described in detail. 5H-BN is energetically more favorable than other polytypes with the exception of 3C-BN in the previous study.[14] We did not treat 6H-BN in the previous study.[14] The calculation of 6H-BN was done to compare the results with 5H-BN.

Silicon-carbide (SiC) has various polytypes.[5–7] Although SiC polytypes have been intensively studied experimentally and theoretically,[18–29] there are few studies of 5H-SiC available.[30–33] 5H-SiC was calculated using a tight-binding method in a theoretical study.[33] Of the various polytypes, 2H-, 3C-, 4H-, and 6H-SiC have been studied extensively in theoretical studies.[19–29] In theory, 4H-SiC is the most stable although total energy differences among polytypes are quite small, within approximately 10 meV.

2H- and 3C-aluminum nitride (AlN) are wide band gap materials. 2H-AlN is a stable phase and 3C-AlN is a metastable phase.[34] Few experiments have been done on 4H-AlN.[35–37] Very recently, 6H-AlN has been synthesized.[38] The electronic properties of 4H- and 6H-AlN have been calculated by Liu and Ni.[39] No experimental and theoretical studies of 5H-AlN have been done. Previous studies have shown in the band gaps of the electronic band structures of BN and SiC polytypes to be indirect. It is expected that band gaps of 4H-, 5H-, and 6H-AlN may be direct because that of 2H-AlN is direct.[34,40–43] Therefore, we have investigated their electronic band structures in this study.

We calculated the electronic and lattice properties of 2H, 3C (= 3H), 4H, 5H, and 6H polytypes (BN, SiC, and AlN) using the first-principles molecular dynamics (FPMD) method in this study. We also calculated their energetical stabilities. Hexagonality, which is defined at the end of §3, is an important parameter to discuss the stabilities of polytypes. We compared the electronic and lattice properties of BN polytypes with those of SiC and AlN polytypes and we calculated the electronic band structures of BN, SiC, and AlN polytypes in order to obtain their valence band maximum (VBM), conduction band minimum (CBM), and minimum (direct) band gaps. In addition, sp^2-bonded hexagonal phases of BN, SiC, and AlN (*h*-BN,[44] *h*-SiC, and *h*-AlN) were treated to compare them with their sp^3-bonded polytypes.

The 6H polytype has two crystal structures.[7] One has a $P6_3mc$ symmetry, which is most commonly accepted, and the other has a $P3m1$ symmetry. We found in this study that the latter of two structures in AlN is more stable than the more widely accepted 6H structure.

2. Method of Calculation

The present calculation is based on the local density approximation (LDA) in density functional theory[45,46] (DFT) with the von Barth and Hedin (BH) interpolation formula[47] for the exchange-correlation. For SiC polytype, the Wigner interpolation formula[48] for the exchange-correlation was also used in order to compare with the results using BH. The norm-conserving pseudopotential (BHS-type)[49] was used for Si. The optimized pseudopotentials by Troullier and Martins (TM)[50,51] are used for Al, B, C, and N. Nonlocal parts of the pseudopotentials are transformed to the Kleinman–Bylander separable forms[52] without ghost bands. A partial core correction (PCC)[53] is considered for the Al pseudopotential.

Mesh sizes of sampling k-points in an irreducible Brillouin zone (BZ) for 2H-, 3H-, 4H-, 5H-, 6H-, 3C-, and *h*-BN (SiC, AlN) are $12 \times 12 \times 8$, $12 \times 12 \times 4$, $12 \times 12 \times 8$, $12 \times 12 \times 4$, $12 \times 12 \times 2$, $8 \times 8 \times 8$, and $12 \times 12 \times 8$ ($18 \times 18 \times 12$ for *h*-BN[44]), respectively. A convergence of lattice parameters is sufficient at the $12 \times 12 \times 4$ ($12 \times 12 \times 2$ for 6H) mesh because all calculated polytypes are non-metallic. The wave function is expanded in plane waves and the cutoff energy is 144 Ry in all calculated phases. As for the cutoff energy, a sufficient convergence in *h*-BN was obtained at 144 Ry in the previous study.[44] A structural optimization of internal parameters was performed using Hellmann–Feynman forces in the unit cell. Our criterion for optimizing the internal coordinates is that the maximum force acting on each atom should be less than 2.0×10^{-4} Ry/bohr, and our criterion for optimizing the unit cell surfaces is that the maximum stress[54] acting on each unit cell surface should be less than 0.03 GPa.

3. Crystal Structure

In this study, we consider the 2H, 3H (= 3C), 4H, 5H, and 6H polytypes which are all hexagonal except for the 3C structure. The 3C structure is cubic (zinc-blende). 3H-BN(ABC) and one 5H-BN(ABCBC) stacking sequence are shown in Fig. 1. A hexagonal layer is occupied by B (N) atoms and B- and N-layers stack alternately. Three atomic positions, (x, y)[5] of (0, 0) as P, (1/3, 2/3) as Q, and (2/3, 1/3) as R, can be placed by a B or N atom on the (x, y)-plane. It is defined as successive B- and N-layers (B–N bilayer) at (0, 0) as A, (1/3, 2/3) as B, and (2/3, 1/3) as C (Fig. 1). (0, 0) is the original point. 3H-BN is structurally equal to 3C-BN. The direction of the [111]-axis in 3C-BN corresponds to that of the *c*-axis in 3H-BN. Although it is possible to consider a smaller primitive unit cell in 3H-BN, we treat a larger unit cell with the ABC stacking sequence, as in the 3H polytype, in this study. These features are the same for SiC and AlN. Two 6H structures are shown below in Fig. 2. The number of atoms/layers ($N_{\mathrm{atom}}/N_{\mathrm{layer}}$) and structural symmetries for the 2H, 3C, 3H, 4H, 5H, and 6H polytypes are tabulated in Table I. The numbers (N_{third}, p) of the third-neighbor cation–anion pairs and cation–anion bilayers, and hexagonality, which are mentioned later in detail, are also tabulated in Table I. In polytypes, a tetrahedral structure is formed by cation and anion atoms in the unit cell. The numbers of the first-neighbor and second-neighbor atoms are four and twelve per one atom in the ideal tetrahedral structure. The

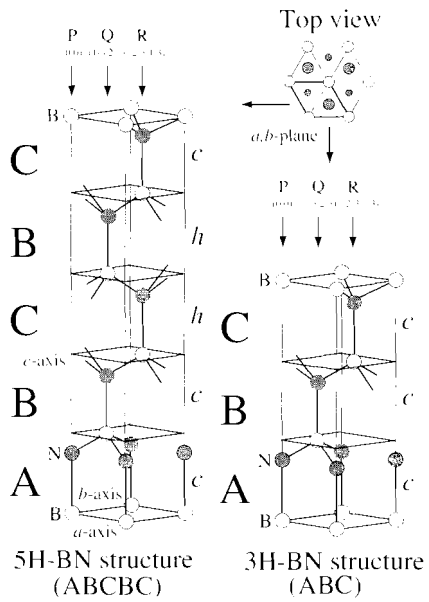

Fig. 1. Crystal structures (unit cells) of 3H-BN and 5H-BN, and top view. P, Q, and R are possible atomic positions. The cubic and hexagonal characters of the BN bilayers are indicated by *c* and *h*.

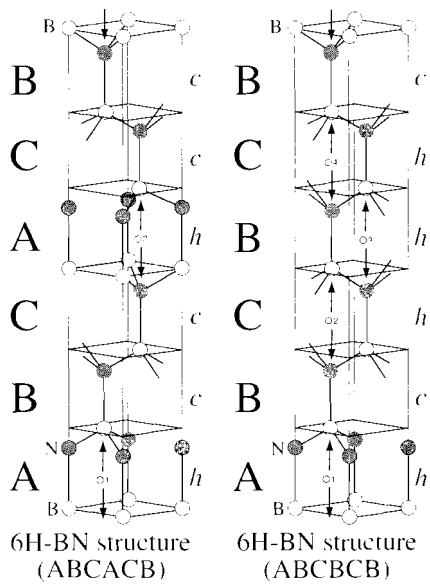

Fig. 2. Crystal structures (unit cells) of 6H-BN as ABCACB and ABCBCB. The cubic and hexagonal characters of the BN bilayers are indicated by *c* and *h*. The third-neighbor B–N atoms are indicated by arrows. ○1, ○2, ○3, and ○4 indicate the third-neighbor B–N pairs in Table V.

first-neighbor atoms are a cation–anion pair and the second-neighbor atoms are the cation–cation or anion–anion pair. Although polytypes have similar tetrahedral bonds up to the second-neighbor in the ideal tetrahedral structure, it is possible to consider different bonds in the third-neighbor which are a cation–anion pair. We treat the shortest third-neighbor cation–anion pair in this study. 2H, 3H, 4H, 5H, and 6H structures have internal parameters along the *c*-axis in the unit cell as indicated by "○" in Table I. In this study, polytypes include the 3C cubic structure and do not include sp^2-bonded hexagonal structures such as *h*-BN,

Table I. Symmetries of 6H-BN(ABCACB), 6H-BN(ABCBCB), 5H-BN(ABCBC), 4H-BN(ABCB), 3H-BN(ABC), 2H-BN(AB), 3C-BN, and *h*-BN. N_{atom} and N_{layer} are the numbers of atoms and hexagonal layers in the unit cell, respectively. N_{third} is the number of third-neighbor B–N pairs parallel to the *c*-axis in the unit cell. *p* is the number of B–N bilayers in the unit cell. "" indicates an existence of internal parameters. *H* indicates hexagonality. These properties are the same for SiC and AlN phases.

	Symmetry	N_{atom}/N_{layer}	N_{third}	*p*	Internal	*H* (%)
6H-BN(ABCACB)	$P6_3mc$	12/12	2	6	""	33
6H-BN(ABCBCB)	$P\bar{3}m1$	12/12	4	6	""	67
5H-BN(ABCBC)	$P\bar{3}m1$	10/10	2	5	""	40
4H-BN(ABCB)	$P6_3mc$	8/8	2	4	""	50
3H-BN(ABC)	$P\bar{3}m1$	6/6	0	3	""	0
2H-BN(AB)	$P6_3mc$	4/4	2	2	""	100
3C-BN	$F\bar{4}3m$	2/—	0	—	—	0
h-BN	$P6_3/mmc$	4/2	—	—	—	—

h-SiC, and *h*-AlN. Rhombohedral lattice structures, impurities, defects, stacking faults and intercalation are not considered in this study.

The 2H, 3H, and 4H polytypes are determined uniquely.[7,14] The 5H polytype consists of 10 hexagonal layers (= five cation–anion bilayers) in the unit cell. We have demonstrated the existence of this structure in the previous study.[14] More specifically it is possible to consider 30 stacking sequences in the 5H-BN structure. This sequence was obtained using circular permutation of AABBC, AACCB, and ABBCC as starting sequences. ABBCC is equal to ACCBB. The successive letters as AA, BB, and CC are forbidden in the stacking sequences. Other starting sequences are impossible because the double letter AA (BB, CC) cannot be excluded from them. In AABBC, four stacking sequences are possible: A-BCAB, A-BACB, A-BABC, and A-CBAB. In the same way, four stacking sequences are possible in AACCB. In ABBCC, two stacking sequences are possible (A-BCBC and A-CBCB). Consequently, there are 30 possible total stacking sequences from the above 10 stacking sequences and their cyclic shift of letters is A → B → C. We have shown that possible 30 stacking sequences are the same structure relocating a periodic boundary or original point in the unit cell.[14] The same can be done for 5H-SiC and 5H-AlN.

The 6H polytype has 54 possible stacking sequences. This number was obtained using the circular permutation of AABBCC, AAABBC, AAACCB, AABBBC, AACCCB, ABBBCC, and ACCCBB as starting sequences. AABBCC is equal to AACCBB. The double letters AA, BB, and CC are also impossible in these stacking sequences. Other starting sequences are impossible because the double letter AA (BB, CC) can not be excluded from them. AAABBB and AAACCC have no possible stacking sequences with the exception of the 2H structures such as ABABAB and ACACAC. The numbers of possible stacking sequences from above starting sequences are 6, 3, 3, 2, 2, 1, and 1, respectively. Therefore, the possible total number of stacking sequences is 54 from above 18 stacking sequences and their cyclic shift of letters is A → B → C. It is possible to consider two crystal structures in the 6H polytype.[7] These 54 stacking sequences can be classified into two groups: One is 18 stacking sequences from AABBCC and the other is 36 stacking sequences from AAABBC, AAACCB, AABBBC, AACCCB, ABBBCC, and ACCCBB. The former 18 stacking sequences from AABBCC are the same structure created by relocating the periodic boundary or original point in the unit cell. We use the stacking sequence "ABCACB" to refer to this structure. Moreover, the latter 36 stacking sequences are the same structure created by relocating the periodic boundary, A → C and C → A, or original point in the unit cell. We use the stacking sequence "ABCBCB" to refer to this structure. Crystal symmetries of ABCACB and ABCBCB are $P6_3mc$ and $P\bar{3}m1$, respectively. Their crystal structures are shown in Fig. 2. ABCACB is the most commonly accepted stacking sequence. Most experimental and theoretical studies of the 6H polytype treated basically the most accepted 6H structure as ABCACB with the exception of a few works.[7,19]

The cubic (*c*) and hexagonal (*h*) characters of the BN (SiC, AlN) bilayers are shown in Figs. 1 and 2 as indicated by *c* and *h*. Hexagonality (*H*)[22,23,26] is the ratio of the number of *h* character and the total number of *c* and *h* characters in the unit cell. The hexagonalities (%) of 2H, 3H (= 3C), 4H, and 5H polytypes are 100, 0, 50, and 40, respectively. The hexagonalities (%) of ABCACB and ABCBCB in the 6H polytype are 33 and 67%, edited respectively.

4. Results and Discussion

4.1 Lattice properties

The optimized lattice properties and hexagonalities (%) of BN, SiC, and AlN polytypes are tabulated in Tables II–IV, respectively. Their total energies per B_2N_2 (Si_2C_2, Al_2N_2) are also tabulated. Comparable lattice constants *a* and *c* agree well with the experimental results in Tables II–IV. Lattice constants *a* and *c* of 6H-BN in experiment[17] are 12.44 and 2.50 Å, respectively, the crystal symmetry of which has not been determined. These values agree with the calculated values of 6H-BN(ABCACB) and 6H-BN(ABCBCB). Calculated lattice constants *c* of BN polytypes are always slightly underestimated in comparison with experimental values. Therefore, lattice constant *c* (12.411 Å) of 6H-BN(ABCACB) is closer to the experimental value than that of 6H-BN(ABCBCB). Lattice constants *a* and *c* of SiC polytypes using the BH formula are slightly smaller than those using the Wigner interpolation formula and experimental values from Table III. Although the agreement of theoretical and experimental lattice constants is better using Wigner than using BH, the electronic properties and order of the total energies are qualitatively invariant in both LDA types (BH, Wigner) as mentioned in the next subsection. The lattice constants of 2H-, 3H-, 4H-, and 6H(ABCACB)-AlN agree well with the theoretical results[39] with DFT–GGA calculations. Lattice constants *a* and *c*/*p* of BN, SiC, and AlN are almost invariant in each polytype. *p* is the number of cation–anion bilayers in the unit cell. Lattice constants *a* and *c*/*p* of BN are smaller than those of SiC and AlN. Values of lattice constants *a* and *c*/*p* for SiC and AlN are nearly equal to each other within approximately 0.1–0.2 Å. Bulk moduli *B* of 5H-BN, 5H-SiC, and 5H-AlN and their pressure derivatives *B'* are 403 GPa, 213 GPa, 207 GPa, and 3.47, 3.74, 3.78, respectively. These values are

Table II. Optimized lattice constants a and c, c/p, and the c/a ratios of 6H-BN(ABCACB), 6H-BN(ABCBCB), 5H-BN(ABCBC),[14] 4H-BN(ABCB), 3H-BN(ABC), 2H-BN(AB), 3C-BN, and h-BN.[44] p is the number of B–N bilayers in the unit cell. Experimental results of 6H-, 5H-, 2H-, 3C-, and h-BN are also tabulated. E_{tot} is the total energy per B_2N_2. ΔE indicates the total energy difference (meV) from 3C-BN. BH indicates the LDA type.[47] H indicates hexagonality.

BH	c (Å)	c/p (Å)	a (Å)	c/a	E_{tot} (eV)	ΔE (meV)	H (%)
6H-BN(ABCACB)	12.411	2.069	2.522	4.921	−710.59556	20	33
6H-BN(ABCBCB)	12.451	2.075	2.519	4.943	−710.57003	46	67
5H-BN(ABCBC)[14]	10.349	2.070	2.522	4.104	−710.58917	26	40
4H-BN(ABCB)	8.287	2.072	2.521	3.288	−710.58435	31	50
3H-BN(ABC)	6.187	2.062	2.526	2.449	−710.61563	—	0
2H-BN(AB)	4.164	2.082	2.516	1.655	−710.54046	75	100
3C-BN	3.572	—	3.572	1.000	−710.61563	0	0
h-BN[44]	6.568	—	2.478	2.651	−710.48931	126	—
6H-BN(Exp[17])	12.44	—	2.500	4.976	—	—	—
5H-BN(Exp[14])	10.407	—	2.528	4.117	—	—	—
2H-BN(Exp[13])	4.22	—	2.553	1.653	—	—	—
3C-BN(Exp[13])	3.616	—	3.616	1.000	—	—	—
h-BN(Exp[13])	6.656	—	2.504	2.658	—	—	—

Table III. Optimized lattice constants a and c, c/p, and the c/a ratios of 6H-SiC(ABCACB), 6H-SiC(ABCBCB), 5H-SiC(ABCBC), 4H-SiC(ABCB), 3H-SiC(ABC), 2H-SiC(AB), 3C-SiC, and h-SiC. p is the number of Si–C bilayers in the unit cell. Experimental results of 6H-, 4H-, 2H-, and 3C-SiC are also tabulated. E_{tot} is the total energy per Si_2C_2. ΔE indicates the total energy difference from 4H-SiC. BH and Wigner indicate the LDA types,[47,48] respectively. H indicates hexagonality.

BH	c (Å)	c/p (Å)	a (Å)	c/a	E_{tot} (eV)	ΔE (meV)	H (%)
6H-SiC(ABCACB)	14.948	2.491	3.047	4.906	−535.95822	0.31	33
6H-SiC(ABCBCB)	14.966	2.494	3.045	4.914	−535.95352	5.0	67
5H-SiC(ABCBC)	12.461	2.492	3.046	4.090	−535.95401	4.5	40
4H-SiC(ABCB)	9.971	2.493	3.046	3.273	−535.95853	0	50
3H-SiC(ABC)	7.466	2.489	3.048	2.449	−535.95450	—	0
2H-SiC(AB)	4.995	2.498	3.044	1.641	−535.94416	14.4	100
3C-SiC	4.311	—	4.311	1.000	−535.95452	4.0	0
h-SiC	4.662	—	3.132	1.488	−534.15176	1807	—
Wigner	c (Å)	c/p (Å)	a (Å)	c/a	E_{tot} (eV)	ΔE (meV)	H (%)
6H-SiC(ABCACB)	15.115	2.519	3.080	4.908	−526.19838	0.14	33
6H-SiC(ABCBCB)	15.136	2.523	3.078	4.917	−526.19297	5.6	67
5H-SiC(ABCBC)	12.602	2.520	3.080	4.092	−526.19423	4.3	40
4H-SiC(ABCB)	10.084	2.521	3.079	3.275	−526.19852	0	50
3H-SiC(ABC)	7.548	2.516	3.082	2.449	−526.19530	—	0
2H-SiC(AB)	5.053	2.527	3.077	1.642	−526.18294	15.6	100
3C-SiC	4.358	—	4.358	1.000	−526.19533	3.2	0
h-SiC	4.890	—	3.147	1.554	−524.40233	1796	—
6H-SiC(Exp[59])	15.12	—	3.081	4.907	—	—	—
4H-SiC(Exp[58])	10.0517	—	3.073	3.271	—	—	—
3C-SiC(Exp[57])	4.360	—	4.360	1.000	—	—	—
2H-SiC(Exp[56])	5.052	—	3.079	1.641	—	—	—

consistent with other BN, SiC, and AlN polytypes. Atomic displacements of internal parameters from the ideal positions for the 3H, 4H, 5H, and 6H polytypes are quite small, within approximately 0.1% of lattice constant c. Those of 2H polytypes are small within approximately 1.0% of lattice constant c. It is possible to neglect the influence of displacements of internal atoms on the tetrahedral lattice properties with the exception of AlN polytypes. In 3H polytypes for BN, SiC, and AlN, no internal atoms move from their ideal positions without DFT–LDA calculation errors although they can move along the c-axis in the $P3m1$ symmetry.

4.2 *Total energies and stability*

From Tables II–IV, the order of the calculated total energies of the BN, SiC, and AlN polytypes are as follows. The total energies of the BN polytypes are in the order of 3C (0%) < 6H(ABCACB) (33%) < 5H (40%) < 4H (50%) <

Table IV. Optimized lattice constants a and c, c/p, and the c/a ratios of 6H-AlN(ABCACB), 6H-AlN(ABCBCB), 5H-AlN(ABCBC), 4H-AlN(ABCB), 3H-AlN(ABC), 2H-AlN(AB), 3C-AlN, and h-AlN. p is the number of Al–N bilayers in the unit cell. Experimental results of 4H-, 2H-, and 3C-AlN are also tabulated. As for lattice constants a of 4H-AlN,[37] $2d_{11\bar{2}0}$ is 3.105 Å and $(2/\sqrt{3})d_{10\bar{1}0}$ is 3.079 Å in parentheses. Theoretical results (Th) of 6H-, 4H-, 3H-, and 2H-AlN are also tabulated. E_{tot} is the total energy per Al_2N_2. ΔE indicates the total energy difference from 2H-AlN. BH indicates the LDA type.[47] H indicates hexagonality.

BH	c (Å)	c/p (Å)	a (Å)	c/a	E_{tot} (eV)	ΔE (meV)	H (%)
6H-AlN(ABCACB)	15.120	2.520	3.102	4.875	−671.66201	55	33
6H-AlN(ABCBCB)	15.059	2.510	3.108	4.846	−671.68783	29	67
5H-AlN(ABCBC)	12.590	2.518	3.103	4.058	−671.66655	50	40
4H-AlN(ABCB)	10.061	2.515	3.105	3.241	−671.67513	41	50
3H-AlN(ABC)	7.586	2.529	3.097	2.449	−671.63793	—	0
2H-AlN(AB)	4.994	2.497	3.115	1.603	−671.71654	0	100
3C-AlN	4.380	—	4.380	1.000	−671.63794	79	0
h-AlN	4.159	—	3.305	1.258	−671.30916	407	—
6H-AlN(Th[39])	15.1330	—	3.1042	4.875	—	—	—
4H-AlN(Th[39])	10.0697	—	3.1067	3.241	—	—	—
3H-AlN(Th[39])	7.5913	—	3.1001	2.449	—	—	—
2H-AlN(Th[39])	4.9956	—	3.1165	1.603	—	—	—
4H-AlN(Exp[37])	10.032	—	3.105 (3.079)	3.231 (3.258)	—	—	—
3C-AlN(Exp[60])	4.37	—	4.37	1.000	—	—	—
2H-AlN(Exp[61])	4.980	—	3.110	1.601	—	—	—

6H(ABCBCB) (67%) < 2H (100%). The total energies of SiC polytypes are in the order of 4H (50%) < 6H-(ABCACB) (33%) < 3C (0%) < 5H (40%) < 6H(ABCBCB) (67%) < 2H (100%). The total energies of AlN polytypes are in the order of 2H (100%) < 6H(ABCBCB) (67%) < 4H (50%) < 5H (40%) < 6H(ABCACB) (33%) < 3C (0%). Values in parentheses are hexagonalities (%). The total energy of the BN polytype increases with increasing hexagonality. In contrast, the total energy of the AlN polytype decreases with increasing hexagonality. c/p corresponds to a height of one tetrahedron in the unit cell. The c/p values for the BN and SiC polytypes increase with increasing hexagonality and that of the AlN polytype decreases with increasing hexagonality from Tables II–IV. For the BN and AlN polytypes, c/p is smaller at lower total energies. There seems to be little correlation among the total energy, hexagonality, and c/p in SiC polytypes. Energetically, 3C-BN (= 3H-BN), 4H-SiC, and 2H-AlN are most stable in each calculated BN, SiC, and AlN phase, respectively. Total energies of h-BN, h-SiC, and h-AlN, which are sp^2-bonded compounds, are highest in each BN, SiC, and AlN phase. Total energy differences, which are denoted by ΔE, are also tabulated in Tables II–IV. The total energy differences between the 3C and 3H polytypes are quite small, within 0.03 meV since the 3C structure is equal to the 3H structure. These small differences originate from the errors of the DFT–LDA calculations. The largest total energy differences of SiC polytypes are 14.4 meV (BH) and 15.6 meV (Wigner) and those of BN and AlN polytypes are 75 meV (BH) and 79 meV (BH), respectively. Although the total energies of 2H-BN and 3C-AlN are highest in each polytype, they are synthesized in experiment.[13,60] The total energy differences between h-SiC and 2H-SiC are 1.79 eV (BH) and 1.78 eV (Wigner), respectively, which are quite larger than those between 2H-BN–h-BN and 3C-AlN–h-AlN. The total energy differences of 4H-SiC and 6H-SiC(ABCACB) are 0.14 meV (Wigner) and 0.31 meV (BH), respectively. These values are quite small and are within the errors of DFT–LDA calculations. This trend is quantitatively similar to other theoretical results.[33] The total energy order of SiC polytypes is invariant in two LDA types (BH[47] and Wigner[48]) despite the energy differences among polytypes (within approximately 10 meV). This energy order agrees with other theoretical results[33] with the exception of 5H-SiC. The total energy of 5H-SiC obtained by the tight-binding method[33] is lower by 0.7 meV/SiC (= 1.4 meV/Si_2C_2) than that of 3C-SiC. In this study, the total energy of 5H-SiC is higher by 1.1 meV/Si_2C_2 than that of 3C-SiC. 6H-BN(ABCACB) is more favorable than 5H-BN (Table II). In 6H-BN and 6H-SiC, the ABCACB stacking sequence is energetically more favorable than the ABCBCB stacking sequence, but 6H-AlN(ABCBCB) is more favorable than 6H-AlN(ABCACB). Lattice constants c and c/p of 6H-BN(ABCACB) and 6H-SiC(ABCACB) are slightly smaller than those of 6H-BN(ABCBCB) and 6H-SiC(ABCBCB), respectively. Lattice constant c and c/p of 6H-AlN(ABCACB) are slightly larger than those of 6H-AlN(ABCBCB). These differences in lattice constants c between ABCACB and ABCBCB are within 1%.

Atomic radii and electronegativity of B, N, Si, C, and Al are 0.88, 0.70, 1.17, 0.77, and 1.26 Å, and 2.0, 3.0, 1.8, 2.5, and 1.5,[55] respectively. A difference of atomic radii between Al and N is larger than that between B and N since the atomic radius of Al is larger than that of B. The difference of atomic radii between B and N is smallest in BN, SiC, and AlN. The sums of atomic radii as B + N, Si + C, and Al + N are 1.58, 1.94, and 1.96 Å, respectively, which agree with the bond lengths of BN, SiC, and AlN bilayers (1.56, 1.88, and 1.90 Å, respectively) in the 2H polytype. The bond length of the BN bilayer is smallest and implies a strong covalent binding. This is consistent with the large bulk modulus of BN (403 GPa for 5H-BN). An ionicity of AlN is larger than those of BN and SiC because the difference of electronegativity between Al and N is largest. Polytypes have internal parameters with the exception of 3C. Optimized

Table V. Internal parameters of B (Al) and N atoms along the c-axis for 2H-BN(AB), 2H-AlN(AB), 6H-BN(ABCACB), 6H-BN(ABCBCB), 6H-AlN(ABCACB), and 6H-AlN(ABCBCB). These parameters are normalized as for lattice constant c. Δu and Δz are differences between optimized and ideal internal parameters. ABCACB (ABCBCB) is AaBbCcAaCcBb (AaBbCcBbCcBb) which is indicated in parentheses as capital (small) letters for B and Al (N). (1.0) and (1.5) in 2H-BN and 2H-AlN means the internal parameters of the upper next unit cell and they are indicated by (○1) and (○2), respectively. "3rd" indicates the third-neighbor cation–anion pair parallel to the c-axis as ○1 (○1)–○1, ○2 (○2)–○2, ○3–○3, and ○4–○4. "Ideal" indicates ideal values of internal parameters. 7/24 is 0.291667, 11/24 is 0.458333, 19/24 is 0.791667, and 23/24 is 0.958333.

	2H-BN(AB)	Δu	3rd	2H-AlN(AB)	Δu	3rd	Ideal
B(Al)(A)	0.0 (1.0)	0	(○1)	0.0 (1.0)	0	(○1)	0.0
B(Al)(B)	0.5 (1.5)	0	(○2)	0.5 (1.5)	0	(○2)	0.0
N(a)	0.3744	-6×10^{-4}	○1	0.3814	64×10^{-4}	○1	0.375
N(b)	0.8744	-6×10^{-4}	○2	0.8814	64×10^{-4}	○2	0.875
	6H-BN(ABCACB)	Δz	3rd	6H-BN(ABCBCB)	Δz	3rd	Ideal
B(A)	0.0	0	—	0.0	0	—	0.0
B(B)	0.1674	7×10^{-4}	○1	0.1669	2×10^{-4}	○1	1/6
B(C)	0.3335	2×10^{-4}	—	0.3328	-5×10^{-4}	—	1/3
B(A)(B)	0.5	0	—	0.5001	1×10^{-4}	○2	1/2
B(C)	0.6674	7×10^{-4}	○2	0.6673	6×10^{-4}	○3	2/3
B(B)	0.8335	2×10^{-4}	—	0.8341	8×10^{-4}	○4	5/6
N(a)	0.1257	7×10^{-4}	—	0.1253	3×10^{-4}	—	1/8
N(b)	0.2920	3×10^{-4}	—	0.2911	-6×10^{-4}	○2	7/24
N(c)	0.4581	-2×10^{-4}	○2	0.4581	-2×10^{-4}	○3	11/24
N(a)(b)	0.6257	7×10^{-4}	—	0.6253	3×10^{-4}	○4	5/8
N(c)	0.7920	3×10^{-4}	—	0.7925	8×10^{-4}	—	19/24
N(b)	0.9581	-2×10^{-4}	○1	0.958265	0.7×10^{-4}	○1	23/24
	6H-AlN(ABCACB)	Δz	3rd	6H-AlN(ABCBCB)	Δz	3rd	Ideal
Al(A)	0.0	0	—	0.0	0	—	0.0
Al(B)	0.1658	-9×10^{-4}	○1	0.1662	-5×10^{-4}	○1	1/6
Al(C)	0.3329	-4×10^{-4}	—	0.3338	5×10^{-4}	—	1/3
Al(A)(B)	0.5	0	—	0.49995	-0.5×10^{-4}	○2	1/2
Al(C)	0.6658	-9×10^{-4}	○2	0.6662	-5×10^{-4}	○3	2/3
Al(B)	0.8329	-4×10^{-4}	—	0.8324	-9×10^{-4}	○4	5/6
N(a)	0.1252	2×10^{-4}	—	0.12605	10.5×10^{-4}	—	1/8
N(b)	0.291643	-0.24×10^{-4}	—	0.2929	12×10^{-4}	○2	7/24
N(c)	0.4587	4×10^{-4}	○2	0.4598	15×10^{-4}	○3	11/24
N(a)(b)	0.6252	2×10^{-4}	—	0.6260	10×10^{-4}	○4	5/8
N(c)	0.791643	-0.24×10^{-4}	—	0.7923	6×10^{-4}	—	19/24
N(b)	0.9587	4×10^{-4}	○1	0.959155	8.2×10^{-4}	○1	23/24

internal parameters of 2H-BN, 2H-AlN, 6H-BN(ABCACB), 6H-BN(ABCBCB), 6H-AlN(ABCACB), and 6H-AlN-(ABCBCB) are tabulated in Table V. The internal parameters are normalized as for lattice constant c. It is defined that the atomic displacements (Δu, Δz) represent the differences of the optimized and ideal internal parameters in the 2H and 6H polytypes. Stability of SiC polytypes has been discussed in the previous study.[22] Third-neighbor cation–anion atoms play a important role in the total energy lowering and stabilities in the SiC polytypes.[22] The third-neighbor cation–anion pairs of the 2H and two 6H structures which are placed in the adjacent cation and anion atoms parallel to the c-axis in the unit cell are also tabulated by ○1 (○1)–○1, ○2 (○2)–○2, ○3–○3, and ○4–○4 in Table V. The third-neighbor cation–anion pairs indicated by ○1, ○2, ○3, and ○4 in the 6H structures are shown in Fig. 2. From Fig. 2, the third-neighbor cation–anion pair is at the hexagonal character (h) of the cation–anion bilayer in the unit cell. We do not consider other types of third-neighbor atoms in this study. The third-neighbor cation–anion pair treated in this study is the shortest of the possible third-neighbor cation–anion pairs. In the 2H polytype, all anion (cation) atoms have third-neighbor cation (anion) atoms. The third-neighbor N atoms in the next upper unit cell, which are denoted by (1.0) and (1.5), are on top of the B (Al) atoms in the 2H polytype. There are no third-neighbor cation–anion pairs in the 3C (= 3H) polytype. There are two third-neighbor cation–anion pairs in 6H-BN(ABCACB) and 6H-AlN(ABCACB) and four in 6H-BN(ABCBCB) and 6H-AlN(ABCBCB). There are two third-neighbor cation–anion pairs in the 2H, 4H, and 5H polytypes. These numbers (N_{third}) are tabulated in Table I. It is found that a ratio of N_{third}/p corresponds to hexagonality in each polytype. From Table V, the anion (N) atoms in 2H-AlN are more closely bonded to the third-neighbor cation (Al) atoms indicated by (○1). In contrast, the anion (N) atoms in 2H-BN are more distantly bonded to the third-neighbor cation (B) atoms indicated by (○1) although the displacements of anion atoms are approximately ten times smaller than those of 2H-AlN. This indicates closer bonding of the first-neighbor B–N pair which corresponds to the BN bilayer although the contraction of the bond length is quite small.

Table VI. The total energies with optimized internal parameters for BN, SiC, and AlN polytypes. "Optimized" means the structural optimization using FPMD. ΔE is a total energy difference between the polytypes with the optimized and ideal atomic positions. BH indicates the LDA type.[47] H indicates hexagonality.

BH	Optimized (eV)	ΔE (meV)	H (%)
2H-BN(AB)	−710.54046	0.14	100
6H-BN(ABCBCB)	−710.57003	1.22	67
4H-BN(ABCB)	−710.58435	1.22	50
5H-BN(ABCBC)	−710.58917	1.38	40
6H-BN(ABCACB)	−710.59556	1.17	33
3C-BN	−710.61563	0.0	0
2H-SiC(AB)	−535.94416	0.37	100
6H-SiC(ABCBCB)	−535.95352	0.44	67
4H-SiC(ABCB)	−535.95853	0.45	50
5H-SiC(ABCBC)	−535.95401	0.26	40
6H-SiC(ABCACB)	−535.95822	0.28	33
3C-SiC	−535.95452	0.0	0
2H-AlN(AB)	−671.71654	14.2	100
6H-AlN(ABCBCB)	−671.68783	5.94	67
4H-AlN(ABCB)	−671.67513	3.51	50
5H-AlN(ABCBC)	−671.66655	2.29	40
6H-AlN(ABCACB)	−671.66201	1.77	33
3C-AlN	−671.63794	0.0	0

This trend is invariant in the 6H structures. The anion atoms and their third-neighbor cation atoms parallel to the c-axis are more closely (distantly) bonded to each other in 6H-AlN (6H-BN).

We have calculated the total energies of BN, SiC, and AlN polytypes with ideal atomic positions using lattice constants a and c in Tables II to IV. The total energies with the structural optimized atomic positions, which are tabulated in Table VI, are lower than those with the ideal atomic positions. The total energy differences between optimized and ideal atomic positions in the SiC polytypes are small and less than 1.0 meV, those in the BN polytypes are approximately 1.0 meV with the exception of 2H-BN, and those in the AlN polytypes are larger than 1.0 meV. These values which are also tabulated in Table VI are small because the displacements of internal atoms are quite small. The total energy orders of the BN, SiC, and AlN polytypes with the ideal atomic positions were found to be invariant in comparison with those with the optimized atomic positions. In the AlN polytypes, the third-neighbor cation–anion pair is electrostatically attractive because of the larger ionicity. The total energies with the optimized and ideal atomic positions in the AlN polytypes decrease with increasing the ratio of N_{third}/p (= hexagonality). The total energy difference (ΔE) of the AlN polytype increases with increasing hexagonality in Table VI. Since the hexagonality of 6H-AlN(ABCBCB) is larger than that of 6H-AlN(ABCACB), the total energy of 6H-AlN(ABCBCB) is lower than that of 6H-AlN-(ABCACB). The 3C structure has no third-neighbor cation–anion pairs. Therefore, no third-neighbor Al–N bonds are in 3C-AlN and its total energy is highest in the AlN polytypes. On the other hand, 3C-BN is most stable due to the strong first-neighbor B–N bonding. There is no advantage of bonding of the third-neighbor B–N atoms since the ionicity of BN is smaller than that of AlN and its covalency is more significant. The bond length of the first-neighbor B–N pair is smaller than those of the SiC and AlN polytypes. This smaller bond length is energetically more favorable in the covalent binding. c/p of the BN polytype, which is related to the bond length, increases with increasing hexagonality. Consequently, the total energy of the BN polytype increases with increasing hexagonality.

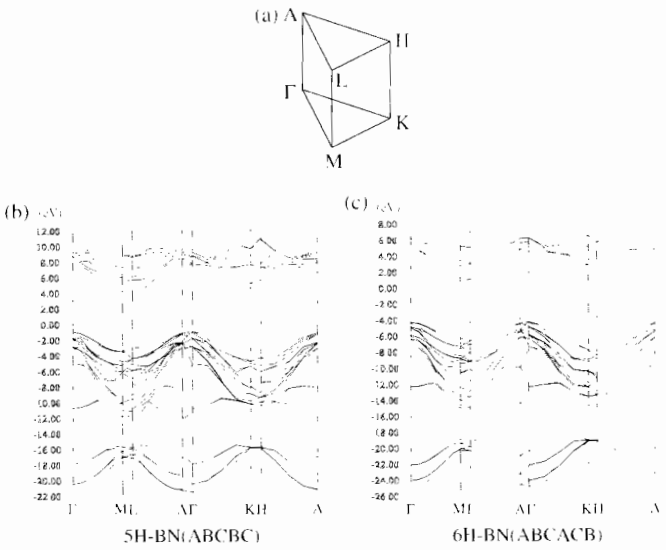

Fig. 3. Hexagonal Brillouin zone and electronic band structures of 5H-BN(ABCBC) and 6H-BN(ABCACB). VBM–CBM of them are Γ–L, Γ–M, respectively.

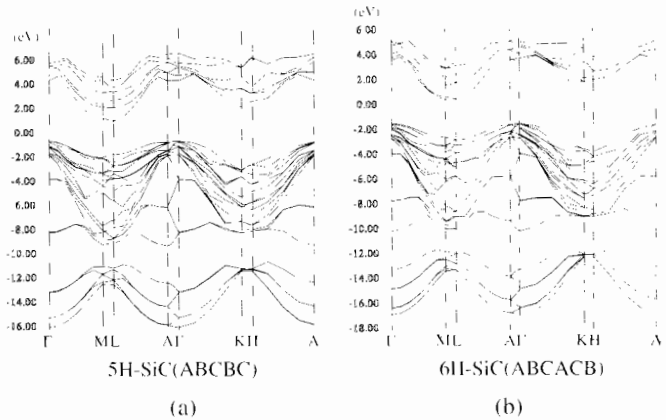

Fig. 4. Electronic band structures of 5H-SiC(ABCBC) and 6H-SiC-(ABCACB). VBM–CBM of them are Γ–L, Γ–U, respectively.

4.3 *Electronic band structures*

All calculated phases are non-metallic with the exception of h-SiC. The hexagonal Brillouin zone is shown in Fig. 3(a). The electronic band structures of 5H-BN and 6H-BN(ABCACB) are shown in Figs. 3(b) and 3(c), those of 5H-SiC and 6H-SiC(ABCACB) are shown in Figs. 4(a) and 4(b), those of 5H-AlN and 2H-AlN are shown in Figs. 5(a) and 5(b), and those of 6H-AlN(ABCACB) and 6H-AlN-(ABCBCB) are shown in Figs. 6(a) and 6(b), respectively. The valence band maximum–conduction band minimum (VBM–CBM) of 5H-BN and 6H-BN(ABCACB) are Γ–L

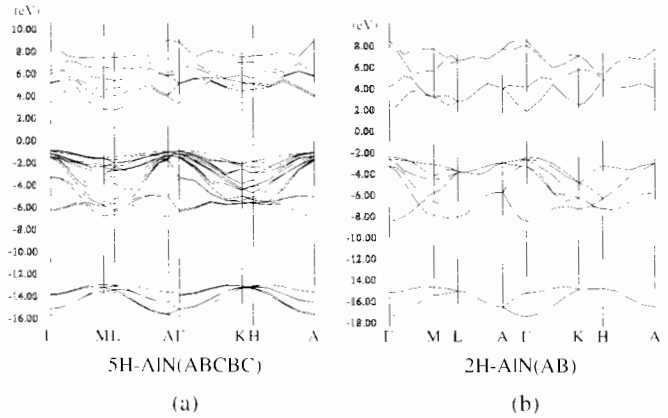

Fig. 5. Electronic band structures of 5H-AlN(ABCBC) and 2H-AlN(AB). VBM–CBM of them are Γ–L, Γ–Γ, respectively.

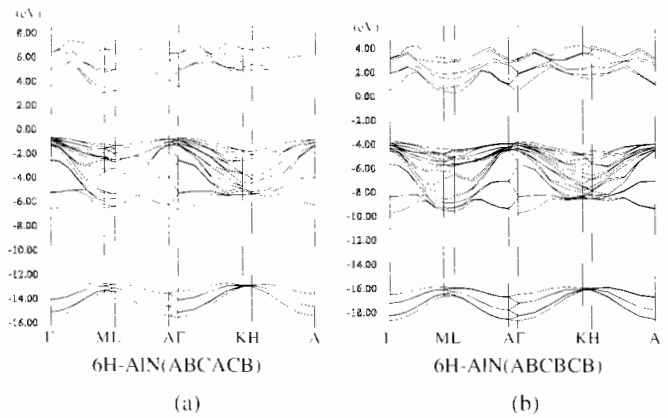

Fig. 6. Electronic band structures of 6H-AlN(ABCACB) and 6H-AlN-(ABCBCB). VBM–CBM of them are Γ–M, Γ–L, respectively.

and Γ–M, respectively. VBM–CBM of 5H-SiC and 6H-SiC(ABCACB) are Γ–L and Γ–U, respectively. The U point is one of the k-points on the M–L line. VBM–CBM of 5H-AlN and 2H-AlN are Γ–L and Γ–Γ, respectively. The band gap of 2H-AlN is direct. VBM–CBM of 6H-AlN(ABCACB) and 6H-AlN(ABCBCB) are Γ–M and Γ–L, respectively. The electronic band structures of 5H- and 6H-AlN are less dispersive than those of the BN and SiC polytypes. Since the numbers of valence electrons in the polytypes are different from each other, their electronic band structures broadly resemble each other although dispersions of individual bands differ slightly between them. Particularly from Figs. 3, 4, and 6, the electronic band structures of 5H and 6H polytypes resemble each other remarkably. In Fig. 6, differences of dispersion, degeneracy and splitting in individual bands of 6H-AlN(ABCACB) and 6H-AlN(ABCBCB) are quite small with the exception of a few cases as CBM. For this reason, it is impossible to discuss the stabilities of 6H-AlN(ABCACB) and 6H-AlN(ABCBCB) based on their electronic band structures.

Electronic properties (VBM, CBM) of BN, SiC, and AlN polytypes are tabulated in Table VII. 3C-BN (3C-AlN), 2H-AlN (2H-BN), 3C-AlN (4.498 Å), and 3C-AlN (4.763 Å) are hypothetical cases in Table VII. The minimum band gap (Δ_1) and minimum direct band gap (Δ_2) are also tabulated in Table VII. It should be noted that these values are underestimated in the DFT–LDA calculations. Totally, the band gap values (Δ_1, Δ_2) of BN are larger than those of SiC and AlN. The band gap values of SiC are smaller than those of BN and AlN. VBM of all polytypes are at the Γ point. This is a typical feature of p-states in sp^3-bonded III–V and VI–VI compounds. CBM of most polytypes are close to the M–L line. VBM and CBM of 3C (= 3H), 4H, 5H, and 6H(ABCBCB) polytypes are invariant in BN, SiC, and AlN. CBM of the 3C polytypes are at the X point which corresponds to the M point[21] in BZ of the 3H polytypes. Most band gaps of BN, SiC, and AlN polytypes are indirect. The band gaps of 2H-AlN and h-AlN are direct. h-SiC is semi-metal. The minimum (direct) band gaps (Δ_1, Δ_2) of 2H-, 3C-, and h-BN agree well with the theoretical results.[10] Although Δ_1 and Δ_2 values (BH) of 2H-, 3C-, 4H-, and 6H-SiC(ABCACB) are smaller by approximately 0.2 to 0.3 eV compared to the theoretical results,[29] their minimum band gaps (Δ_1) agree with theoretical results[21,25,28] (within approximately 0.1 eV). The energy difference between BH and Wigner is approximately 0.1 eV in the SiC polytypes. Although the band gap values of 3C- and 2H-AlN at the Γ point are smaller by approximately 0.4 eV than theoretical results,[40] they agree with other theoretical results[34,41,42] (within approximately 0.1 eV). Since the calculated band gap values are underestimated and smaller by >1 eV than those observed in experiments, disagreement of 0.4 eV with theory is not significant. The Δ_1 values of 4H-AlN and 6H-AlN(ABCACB) agree with the theoretical results.[39] The Δ_1 values of the 3C-BN, 3C-SiC, and 3C-AlN polytypes are smallest in each polytype with the exception of hypothetical cases. Regarding the BN phases, Δ_1 of h-BN is smaller than that of 3C-BN. In SiC polytypes, the largest Δ_1 value (BH) is 2.30 eV for 6H-SiC(ABCBCB). The largest Δ_1 value in AlN polytypes is 4.31 eV for 2H-AlN with the exception of hypothetical cases. The Δ_1 value of 6H-BN(ABCBCB) is 5.6 eV and is largest in the calculated phases in this study. Although this value is inaccurate and 6H-BN(ABCBCB) is energetically more unfavorable than 6H-BN(ABCACB), a wide band gap (>6 eV) may be realized actually. The Δ_1 value of 4H-BN is second largest with 5.52 eV. A difference between the largest and smallest Δ_1 values are more than 1 eV in each phase. 6H-BN(ABCBCB) is not synthesized and there are no experimental and theoretical reports. There seems no correlation between the Δ_1 value and hexagonality.

The band gaps of 4H-, 5H-, and 6H-AlN are indirect although that of 2H-AlN is direct. As for 5H-BN, 5H-SiC, and 5H-AlN, energy differences of the lowest unoccupied conduction bands between the Γ and L points are 3.67, 3.34, and 0.67 eV, respectively. The value (0.67 eV) of 5H-AlN is the smallest of the calculated 5H polytypes. Although the electronic band structures of 6H-AlN(ABCACB) and 6H-AlN(ABCBCB) resemble each other, their CBM are differ at the M and L points, respectively as shown in Table VII. The energy difference of the lowest unoccupied conduction bands between the Γ and L points in 6H-AlN(ABCBCB) is 0.23 eV and is smaller than that of 6H-AlN(ABCACB) (0.56 eV between Γ and M). Since this value (0.23 eV) is small, the direct band gap may be realized in polytypes with a larger number of stacking sequences.

Table VII. Electronic properties of BN, SiC, and AlN polytypes. BH indicates the LDA type.[47] Δ_1 and Δ_2 indicate the minimum band gap and minimum direct band gap (eV), respectively. They are underestimated in the DFT–LDA calculation. Values of SiC polytypes in the parentheses were obtained using the Wigner interpolation formula.[48] 3C-BN (3C-AlN) and 2H-AlN (2H-BN) indicate that equilibrium lattice constants a and c of 3C-AlN and 2H-BN are used, respectively. 3C-AlN (4.498 Å) and 3C-AlN (4.763 Å) indicate the expansion of lattice constants a as 4.498 and 4.763 Å (Equilibrium lattice constant $a = 4.380$ Å), respectively. Parentheses in the Δ_2 column indicate the k-point of the minimum direct band gap. * indicates that the k-point of the minimum direct band gap does not coincide with high symmetry k-points. H indicates hexagonality.

BH		Δ_1 (eV)	Δ_2 (eV)	VBM–CBM	H (%)
6H-BN(ABCACB)	Indirect	5.18	7.26 (M)	Γ–M	33
6H-BN(ABCBCB)	Indirect	5.60	7.89 (U)	Γ–L	67
5H-BN(ABCBC)	Indirect	4.93	7.02 (L)	Γ–L	40
4H-BN(ABCB)	Indirect	5.52	7.63 (M)	Γ–M	50
3H-BN(ABC)	Indirect	4.43	6.94 (*)	Γ–M	0
2H-BN(AB)	Indirect	4.94	8.30 (*)	Γ–K	100
3C-BN	Indirect	4.43	8.83 (Γ)	Γ–X	0
3C-BN (3C-AlN)	Direct	2.75	2.75 (Γ)	Γ–Γ	—
h-BN[44]	Indirect	4.09	4.57 (M)	Near K–M	—
6H-SiC(ABCACB)	Indirect	2.02 (1.93)	3.12 (3.04) (M)	Γ–U	33
6H-SiC(ABCBCB)	Indirect	2.30 (2.19)	3.55 (3.43) (M)	Γ–L	67
5H-SiC(ABCBC)	Indirect	1.74 (1.65)	2.86 (2.77) (L)	Γ–L	40
4H-SiC(ABCB)	Indirect	2.23 (2.13)	3.36 (3.25) (M)	Γ–M	50
3H-SiC(ABC)	Indirect	1.34 (1.27)	2.96 (2.88) (*)	Γ–M	0
2H-SiC(AB)	Indirect	2.16 (2.10)	3.97 (3.82) (M)	Γ–K	100
3C-SiC	Indirect	1.34 (1.27)	4.58 (4.47) (X)	Γ–X	0
h-SiC	Semi metal	—	—	—	—
6H-AlN(ABCACB)	Indirect	3.74	4.27 (M)	Γ–M	33
6H-AlN(ABCBCB)	Indirect	4.06	4.30 (Γ)	Γ–L	67
5H-AlN(ABCBC)	Indirect	3.62	4.17 (L)	Γ–L	40
4H-AlN(ABCB)	Indirect	3.95	4.30 (Γ)	Γ–M	50
3H-AlN(ABC)	Indirect	3.24	4.06 (*)	Γ–M	0
2H-AlN(AB)	Direct	4.31	4.31 (Γ)	Γ–Γ	100
2H-AlN (2H-BN)	Indirect	4.95	7.09 (U)	Near Γ–K	—
3C-AlN	Indirect	3.24	4.29 (Γ)	Γ–X	0
3C-AlN (4.498 Å)	Indirect	3.20	3.57 (Γ)	Γ–X	—
3C-AlN (4.763 Å)	Direct	2.18	2.18 (Γ)	Γ–Γ	—
h-AlN	Direct	3.40	3.40 (Γ)	Γ–Γ	—

We shall discuss how to realize the direct band gap in polytypes. It is important to search wide band gap materials with the ultraviolet region (~6 eV). Particularly, the direct band gap is required because it is expected a higher efficiency of luminescence than the indirect band gap. In Table VII, 3C-BN (3C-AlN), 2H-AlN (2H-BN), 3C-AlN (4.498 Å), and 3C-AlN (4.763 Å) are the hypothetical cases which we calculated in order to discuss the feature of the band gap properties of BN and AlN polytypes because their band gaps are wider than those of SiC. Lattice constant a of 3C-BN (3C-AlN) is used for that of 3C-AlN. This means that the lattice of 3C-BN expands, and this expanded lattice constant corresponds to the negative pressure $P = -76.3$ GPa. The band gap of 3C-BN using this expansion is direct. In the same way, the band gap of 3C-AlN using expanded lattice constant a could be direct. In equilibrium and with expanded lattice constants ($a = 4.380$, $P = 0$ GPa and $a = 4.498$ Å, $P = -14.1$ GPa), their band gaps are still indirect. In $a = 4.763$ Å ($P = -31.3$ GPa), the band gap of 3C-AlN is direct. In contrast, the band gap of 2H-AlN (2H-BN), whose lattice constants a and c are used for those of 2H-BN, becomes indirect. This contraction of lattice constants a and c corresponds to the anisotropic positive pressures $P_{xy} = 424.6$ GPa and $P_z = 337.2$ GPa, although these values are quite large and unusual. The hybridization of s and p-states in the conduction bands becomes weaker by the lattice expansion and s- (p-)states in hybridized conduction bands shift lower (higher). Since the Γ point is the typical minimum of bands originated from s-states, the direct band gap at Γ–Γ is realized. On the other hand, the s–p hybridization becomes stronger by the lattice contraction and the dispersions of s- and p-states in the conduction bands are more complicated. The indirect (direct) band gap changes into the direct (indirect) band gap by the expansion (contraction) of the lattice constant in BN and AlN. Therefore, using ternary compounds as AlXN to expand the lattice constants could be useful to realize the direct band gap. X is a chemical element whose atomic radius is larger than that of Al or N.

On the other hand, VBM of all polytypes are at the Γ point and CBM of most polytypes are at around the M–L line. It could be possible to realize the direct band gap at Γ–Γ or A–A with folding energy bands at the Γ–M or L–A line. For example, we focus on the lowest unoccupied conduction bands of 2H-AlN and 6H-AlN at the M–L, A–Γ, and K–H lines whose lengths correspond to $1/c$ (c: lattice constant) in

real space. The relative positions of the lowest unoccupied conduction bands at the M, L, A, Γ, K, and H points vary with folding each k-line from 2H to 6H as shown in Fig. 5(b) and Figs. 6(a) and 6(b). In the same way, it is necessary to expand the a and/or b lattices [for example: $a \rightarrow 2a$ in real space and $1/a \rightarrow 1/(2a)$ in reciprocal space] in order to fold the energy bands at the Γ–M and/or L–A lines. Impurity or defect doping in polytypes is useful to expand the periodicity of a and b lattices on the a,b-plane. The direct band gap may be realized due to the energy band foldings at the Γ–M and/or L–A lines by impurity or defect doping.

5. Summary

We have calculated the electronic and lattice properties of BN, SiC and AlN polytypes (2H, 3C, 3H, 4H, 5H, and 6H) using FPMD. Hexagonal sp^2-bonded compounds such as h-BN,[44] h-SiC, and h-AlN have been also calculated. Their comparable lattice constants a and c agree well between the experimental and theoretical results. As a result, the order of the calculated total energies of BN, SiC, and AlN polytypes are 3C < 6H(ABCACB) < 5H < 4H < 6H(ABCBCB) < 2H, 4H < 6H(ABCACB) < 3C < 5H < 6H(ABCBCB) < 2H, and 2H < 6H(ABCBCB) < 4H < 5H < 6H(ABCACB) < 3C, respectively. The total energies of the BN and AlN polytypes are related to hexagonality (H) ($= N_{\mathrm{third}}/p$) and c/p. The total energy of the AlN polytype decreases with increasing N_{third}/p ($= H$) due to the larger ionicity. This leads to stabilizing the AlN polytypes with larger hexagonality. In the BN polytypes, covalency is dominant and the 3C structure is most stable. The BN polytype becomes more stable with decreasing hexagonality. In the SiC polytypes, it could not be determined clearly whether or not the total energy is related to hexagonality in this study. The 6H polytype has two crystal structures the ABCACB and ABCBCB stacking sequences, which were also investigated in this study. Their crystal symmetries and hexagonalities (%) are $P6_3mc$ and 33% for ABCACB and $P3m1$ and 67% for ABCBCB, respectively. In 6H-BN and 6H-SiC, the ABCACB stacking sequence is energetically more favorable than the ABCBCB stacking sequence. In contrast, 6H-AlN(ABCBCB) is more favorable than 6H-AlN(ABCACB). Therefore, experimentally synthesized 6H-AlN could have a $P3m1$ crystal symmetry.

We have obtained the electronic band structures, the band gap values, and VBM–CBM of the BN, SiC, and AlN polytypes. The detailed electronic band structures of 4H-BN, 6H-BN, 5H-SiC, 4H-AlN, 5H-AlN, and 6H-AlN which were not investigated previously in detail have been clarified in this study. The electronic band structures of BN, SiC, and AlN polytypes are similar to each other. Most electronic band structures of the BN, SiC, and AlN phases are non-metallic and their band gaps are indirect although those of 2H-AlN and h-AlN are direct (Γ–Γ) and h-SiC is semi-metal. VBM of all calculated polytypes are Γ. CBM of most polytypes are around the M–L line. The minimum band gaps (Δ_1) of the 3C-BN, 3C-SiC, and 3C-AlN are smallest in each polytype and those of 2H-AlN, 6H-BN(ABCBCB), and 6H-SiC(ABCBCB) are largest in each polytype. The largest minimum band gap (Δ_1) is 5.6 eV for 6H-BN(ABCBCB) although the calculated band gap value is underestimated in the DFT–LDA calculation. Since the energy difference between Δ_1 and Δ_2 for 6H-AlN(ABCBCB) is smallest with 0.23 eV in the calculated indirect band gap compounds, the direct band gap may be realized in the larger stacked polytypes. The indirect band gaps of 3C-BN and 3C-AlN change into direct band gaps using hypothetical lattice expansion. Our next task is to investigate lattice and electronic properties of impurity (defect)-doped or ternary polytypes in order to search direct band gap materials.

Acknowledgments

We would like to thank Dr. Y. Yoshimoto for valuable discussions of the electronic band structures. The numerical calculations were performed using the HP xw4400 work-station and the numerical materials simulator (Hitachi SR11000) in NIMS.

1) S. Komatsu, K. Okada, Y. Shimizu, and Y. Moriyoshi: J. Phys. Chem. B **103** (1999) 3289.
2) S. Komatsu, K. Kurashima, H. Kanda, K. Okada, M. Mitomo, Y. Moriyoshi, Y. Shimizu, M. Shiratani, T. Nakano, and S. Samukawa: Appl. Phys. Lett. **81** (2002) 4547.
3) S. Komatsu, A. Okubo, D. Kazami, D. Golberg, Y. Li, Y. Moriyoshi, M. Shiratani, and K. Okada: J. Phys. Chem. B **108** (2004) 5182.
4) S. Komatsu: J. Phys. D **40** (2007) 2320.
5) *International Table for Crystallography*, ed. A. J. C. Wilson and E. Prince (Kluwer, Dordrecht, 2004) Vol. C, Chap. 9.2, pp. 744–765.
6) A. R. Verma and P. Krishna: *Polymorphism and Polytypism in Crystals* (Wiley, New York, 1966).
7) J. E. Iglesias: Acta Crystallogr., Sect. A **62** (2006) 178.
8) K. T. Park, K. Terakura, and N. Hamada: J. Phys. C **20** (1987) 1241.
9) Y. Xu and W. Y. Ching: Phys. Rev. B **44** (1991) 7787.
10) J. Furthmüller, J. Hafner, and G. Kresse: Phys. Rev. B **50** (1994) 15606.
11) A. Janotti, S.-H. Wei, and D. J. Singh: Phys. Rev. B **64** (2001) 174107.
12) K. Shirai, H. Fujita, and H. Katayama-Yoshida: Phys. Status Solidi B **235** (2003) 526.
13) O. Mishima and K. Era: in *Electric Refractory Materials*, ed. Y. Kumashiro (Marcel Dekker, New York, 2000) pp. 495–556, and references therein.
14) K. Kobayashi and S. Komatsu: J. Phys. Soc. Jpn. **76** (2007) 113707.
15) V. F. Britun, A. V. Kurdyumov, and I. A. Petrusha: J. Mater. Sci. **28** (1993) 6575.
16) V. V. Ilyasov, T. P. Zhdanova, and I. Ya. Nikiforov: Phys. Solid State **45** (2003) 816.
17) S. Komatsu: private communications.
18) I. A. Salama, N. R. Quick, and A. Kar: J. Mater. Sci. **40** (2005) 3969.
19) C. Cheng, R. J. Needs, and V. Heine: J. Phys. C **21** (1988) 1049.
20) C. Cheng, V. Heine, and R. J. Needs: J. Phys.: Condens. Matter **2** (1990) 5115.
21) P. Käckell, B. Wenzien, and F. Bechstedt: Phys. Rev. B **50** (1994) 10761.
22) C. H. Park, B. Cheong, K. Lee, and K. J. Chang: Phys. Rev. B **49** (1994) 4485.
23) P. Käckell, B. Wenzien, and F. Bechstedt: Phys. Rev. B **50** (1994) 17037.
24) K. Karch, F. Bechstedt, P. Pavone, and D. Strauch: Phys. Rev. B **53** (1996) 13400.
25) C. Persson and U. Lindefelt: J. Appl. Phys. **82** (1997) 5496.
26) W. R. L. Lambrecht, S. Limpijumnong, S. N. Rashkeev, and B. Segall: Phys. Status Solidi B **202** (1997) 5.
27) F. Bechstedt, P. Käckell, A. Zywietz, K. Karch, B. Adolph, K. Tenelsen, and J. Furthmüller: Phys. Status Solidi B **202** (1997) 35.
28) Z. Jiang, X. Xu, H. Wu, F. Zhang, and Z. Jin: Solid State Commun. **123** (2002) 263.
29) W. Y. Ching, Y. Xu, P. Rulis, and L. Ouyang: Mater. Sci. Eng. A **422** (2006) 147.
30) S. Miyano, S. Sueno, M. Ohmasa, and T. Fujii: Acta Crystallogr., Sect. A **38** (1982) 477, and references therein as for 5H-SiC.

31) JCPDS file number 42-1360, JCPDS International Center for Diffraction Data.
32) Y. Peng, Z. Meng, C. Zhong, J. Lu, W. Yu, and Y. Qian: Mater. Res. Bull. **36** (2001) 1659.
33) N. Bernstein, H. J. Gotsis, D. A. Papaconstantopoulos, and M. J. Mehl: Phys. Rev. B **71** (2005) 075203.
34) P. Jonnard, N. Capron, F. Semond, J. Massies, E. Martinez-Guerrero, and H. Mariette: Eur. Phys. J. B **42** (2004) 351.
35) N. Onojima, J. Suda, T. Kimoto, and H. Matsunami: Appl. Phys. Lett. **83** (2003) 5208.
36) R. Armitage, J. Suda, and T. Kimoto: Appl. Phys. Lett. **88** (2006) 011908.
37) M. Horita, J. Suda, and T. Kimoto: Appl. Phys. Lett. **89** (2006) 112117.
38) D. M. Schaadt, O. Brandt, A. Trampert, H.-P. Schönherr, and K. H. Ploog: J. Cryst. Growth **300** (2007) 127.
39) Z. Q. Liu and J. Ni: Eur. Phys. J. B **59** (2007) 29.
40) C. Stampfl and C. G. Van de Walle: Phys. Rev. B **59** (1999) 5521.
41) C. Persson, A. Ferreira da Silva, R. Ahuja, and B. Johansson: J. Cryst. Growth **231** (2001) 397.
42) R. Ahmed, H. Akbarzadeh, and Fazal-e-Aleem: Physica B **370** (2005) 52.
43) K. Kobayashi: Mater. Trans. **46** (2005) 1094.
44) K. Kobayashi, K. Watanabe, and T. Taniguchi: J. Phys. Soc. Jpn. **76** (2007) 104707.
45) P. Hohenberg and W. Kohn: Phys. Rev. **136** (1964) B864.
46) W. Kohn and L. J. Sham: Phys. Rev. **140** (1965) A1133.
47) U. von Barth and L. Hedin: J. Phys. C **5** (1972) 1629.
48) E. Wigner: Phys. Rev. **46** (1934) 1002.
49) G. B. Bachelet, D. R. Hamann, and M. Schlüter: Phys. Rev. B **26** (1982) 4199.
50) N. Troullier and J. L. Martins: Phys. Rev. B **43** (1991) 1993.
51) K. Kobayashi: Mater. Trans. **42** (2001) 2153.
52) L. Kleinman and D. M. Bylander: Phys. Rev. Lett. **48** (1982) 1425.
53) S. G. Louie, S. Froyen, and M. L. Cohen: Phys. Rev. B **26** (1982) 1738.
54) O. H. Nielsen and R. M. Martin: Phys. Rev. B **32** (1985) 3792.
55) L. Pauling: *The Nature of the Chemical Bond* (Cornell University Press, Ithaca, NY, 1960) pp. 45 and 134.
56) H. Schulz and K. H. Thiemann: Solid State Commun. **32** (1979) 783.
57) *Physics of Group IV and III–V Compounds*, ed. O. Madelung, M. Schulz, and M. Weiss (Springer-Verlag, Berlin, 1982) Landolt–Börnstein, New Series, Group III, Vol. 17, Part A.
58) R. W. G. Wyckoff: *Crystal Structure* (Wiley, New York, 1963).
59) A. H. Gomes de Mesquita: Acta Crystallogr. **23** (1967) 610.
60) *Properties of Group III Nitrides*, ed. J. H. Edgar (IEE, London, 1994) EMIS Datareviews Series.
61) H. Schulz and K. H. Thiemann: Solid State Commun. **23** (1977) 815.